COBEM 2023 27TH INTERNATIONAL CONGRESS OF MECHANICAL ENGENEERING

ABCM Brazilian Society of Mechanical Sciences and Engineering
27th ABCM International Congress of Mechanical Engineering
December 04-08, 2023, Florianópolis-SC, Brazil

COB-2023-2246 ANALYSIS OF A SELF-SUPPORTING HIGH-VOLTAGE POWER TOWER UNDER SEISMIC CONDITIONS WITH THREE-DIMENSIONAL EXCITATIONS

João Lucas Salvador de Araujo
Crystian Daniel de Souza Paz
Federal University of Technology – Paraná
joao.lucas.97@outlook.com
crystianpazprofissional@gmail.com

Gustavo de Miranda Saleme Gidrão
Federal University of Technology – Paraná
gidrao@utfpr.edu.br

Rubia Mara Bosse
Federal University of Technology – Paraná
rubiambosse@utfpr.edu.br

Abstract: *From the social context, high-voltage structures are fundamental in contemporary society due to the transmission of energy and data carried out by them. The collapse of a structure like this can have significant financial impacts, which makes such projects necessary. The current study proposes a methodology for dynamically analyzing a self-supporting high-voltage tower, under three-dimensional seismic excitations, to carry out this analysis, the commercial finite elements software Abaqus was used. An initial analysis is carried out to quantify the total resistance. The simulation methodology developed in this study can be used for decision-making, forecasting repairs, and increasing the structural safety of these important structures for society.*

Keywords: *Self-supporting tower, pushover, dynamic analysis, Abaqus, three-dimensional excitations.*

1. INTRODUCTION

The study suggests a method of implicit dynamic analysis of a self-supporting high-voltage tower under seismic loading. The aim of this analysis is to determine the total resistance of the tower in situations where the earthquake affects it or not. In addition, it is proposed to demonstrate a computational methodology for the modeling of a self-supporting power tower. Analyses of this size are not easily found in the available literature, as cited in Tian et al. (2012), but are fundamental to understanding the possible failure modes of the structure and its residual strength under seismic shaking. To perform this analysis, the commercial finite element software Abaqus was used.

A self-supporting lattice tower with a square base was adapted from the model presented by Gontijo (1994) to perform the analysis. This analysis is performed without the influence of its cables. With a total height of 51.6 m and dimensions defined in Figure 1, the tower contains 1232 bars of beam type B31, as cited by Pan et al. (2021), with a hollow circular section with an outer radius of 10 mm and 6 m thick. The simulated material is ASTM A36 steel with a yield strength of 250 Mpa, according to NBR 8800, Its properties are shown in tables 1, 2 and 3. It should be emphasized that in the study in question the non-linearity of the bars were considered in their perfect plasticity. The mechanical model adopted is as cited by Carlos (2015), truss elements are used, with indelible links and labeled connections.

The data of the three-dimensional base excitations that were obtained from PEER (2015), and four different types of excitations are used, They are Irpinia Earthquake, commented by Bernard and Zollo (1989) with a magnitude of 6.9, Kobe Earthquake, commented by Horwich (2000), with a magnitude of 7.2, Loma Prieta Earthquake, commented by Dietz and Ellsworth (1990) and magnitude of 7.1, and the San Fernando Earthquake, commented by Whitcomb et al. (1973), with a magnitude of 6.4. It should be noted that all the earthquakes mentioned present three acceleration components.

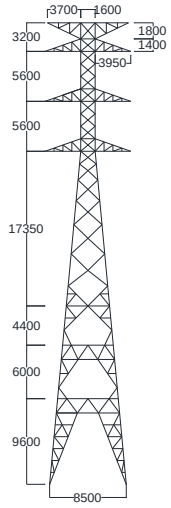

Figure 1. Dimensions of the Tower in millimeters.

Table 1. ASTM A36's Plasticity.

Yield Stress (Mpa)	Plastic Strain
250	0
242.12	0.0189
237.34	0.0255
235.36	0.0422
246.89	0.0607
276.72	0.0834
310.63	0.1094
347.92	0.1350
379.73	0.1581
400.12	0.1823
400.12	0.1993
391.97	0.2175
380.43	0.2298
366.21	0.2417

Table 2. ASTM A36's Elasticity.

Young's Modulus (GPa)	Poisson's Ratio
200	0.3

Table 3. ASTM A36's Density.

Density (Kg/m³)
7500

Initially, the tower structure is modeled using wire edges to create the trusses. After modeling the tower, the properties of the used beam bars are configured, and finally the orientation of the displacement vectors of each bar so that none of the vectors, of the entire tower, coincide in the same direction. For this purpose, the vector (1,1,1) was used. Continuing, the steps necessary to carry out the computational modeling are defined, where it is understood that there is an initial step, then there is the step of the referential pushover in which the links of the structure are crimped, and a displacement of 1 m is applied to the nodes along the tower. After the referential pushover, there is the step of each earthquake used in the study because their durations are different, then an implicit dynamic analysis is performed for each step. To perform the residual pushover analysis, a resting step is configured so that the residual pushover step can then be performed.

With the steps defined, we move on to the boundary conditions, adding the displacements of the pushovers, the links, the accelerations of each earthquake, and the rest conditions. With the help of the Interaction menu, we assign very small inertia to the nodes, thus making them labeled. Then, the mesh is added so that the program can perform the incremental calculations, in Global Seeds an approximate global size of 0.5 is adopted, considering the beam model B31 (A 2-node linear beam in space).

After all the setup is done, a referential nonlinear static pushover analysis, an analysis for each earthquake and an analysis for each earthquake combined with a residual nonlinear static pushover analysis are performed. The baseline three-dimensional excitations for each earthquake are presented in the constituent parts of Graph 1. Collecting the results, the top and base displacements of the structure under the influence of each earthquake are obtained to calculate the roof drift of the stress based on Eq. (1), where Δ_t is the top displacement, Δ_b is the base displacement and h is the total height of the tower. The result obtained is expressed as a percentage (%).

$$Roof\ Drift = (\Delta_t - \Delta_b)/h \quad (1)$$

2. THEORETICAL BACKGROUND

The plasticity model used in this paper follows the guidelines of the ABAQUS Theory Manual (2006):

In section 4.2.1 incremental plasticity is based on some fundamental postulates, which indicates that the elastic-plastic responses of the models created in the software have the same general formula, which is presented in the above-mentioned section. Plasticity models can be written in two ways, namely rate-independent and rate-dependent models. The rate-independent models are those in which the result of the analysis does not depend on the deformation rate, while the rate-dependent models have their result of the analysis depending on the rate that the material is stressed, thus being opposite analyzes. However, as both models have the same shape, their calculations are based on the same technique. To begin with, a basic assumption about elastic-plastic models is made, in which the deformation can be divided into two components, an elastic part, and a plastic part to make up a total deformation.

Graph 1. Basic excitations accelerations: (a) Irpinia Earthquake; (b) Kobe Earthquake; (c) Loma Prieta Earthquake; (d) San Fernando Earthquake.

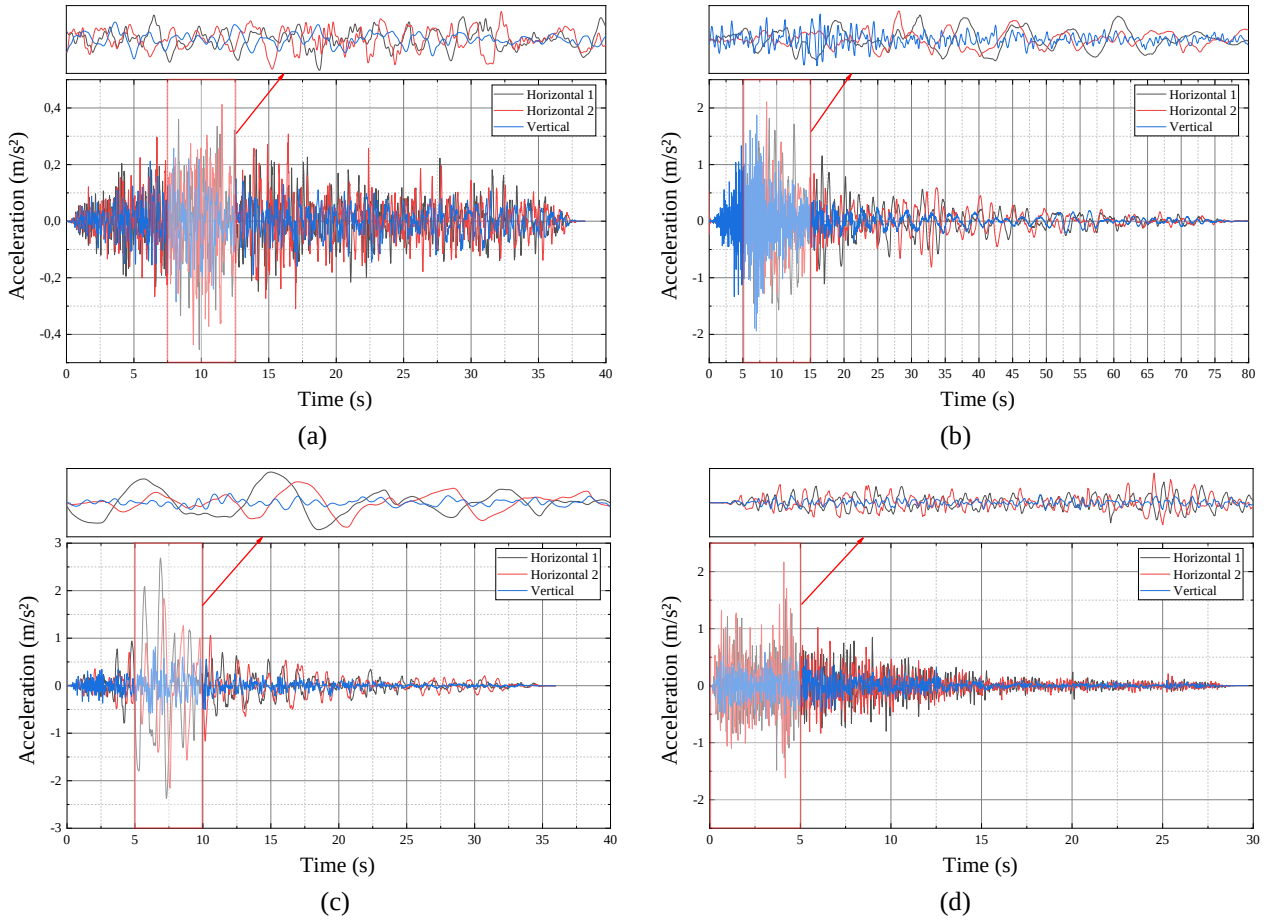

And thus, this division of the deformation into components is given by Eq. (2). Where F represents the total deformation gradient, F^{el} represents the portion of elastic deformation that the model undergoes that makes up the total deformation, and F^{pl} is the portion of plastic deformation to which the model is subjected to occurring and is defined according to Eq. (3).

$$F = F^{el}.F^{pl} \tag{2}$$

$$F^{pl} = [F^{el}]^{-1}.F \tag{3}$$

This analysis composition can be used, in an analogous way, to formulate the plasticity model, for this purpose Eq. (4) shows how the appropriate coefficients are left, where $\mathcal{E}$ here is characterized by the total (mechanical) strain rate that the model is undergoing, $\mathcal{E}^{el}$ is the elastic strain rate and $\mathcal{E}^{pl}$ is the plastic strain rate.

$$\mathcal{E} = \mathcal{E}^{el}.\mathcal{E}^{pl} \tag{4}$$

The demonstration of this concept is duly exposed in item 1.4.4 of this same manual, so that Eq. (4) is a consistent approximation of Eq. (2) when the elastic stresses are infinitesimal, besides when the stress rate used in Eq. 4 is the strain rate of Eq. (5):

$$\mathcal{E} = sym[\partial v/\partial x] \tag{5}$$

As a strain rate is used to define the total rate in Eq. (4), it is used in all plasticity models implemented in Abaqus. The elastic response of the analyzed model is usually a small part of the problem, in fact, the case of the analysis goes as follows: plasticity models are suitable for metal, solids and concrete, for example, and the elastic part presented, in the examples of materials cited, represents a small percentage of the total strain that the part undergoes.

For several of the plasticity models provided in the software, the elasticity is linear, so the stress energy density potential has a very simple form. Also, the rate-independent plasticity models and one of the rate-dependent models have a certain region that only shows elastic responses. Then the yield function, f, defines the boundary for this purely elastic response region is described as in Eq. (6). Where θ is the temperature, H_α is defined by a set of hardening parameters, the index α is simply to indicate that several hardening parameters may occur, and its range of application is defined from the chosen plasticity model. We have σ, which is obtained from the derivative of the energy density potential of the elastic stress (U) defined in Eq. (7). The hardening parameters vary according to the model adopted to allow it to represent part of the complexity of the plastic response of materials. Some models do not use these parameters, others use only 1 parameter, and others use several parameters to perform the analysis. The models provided in Abaqus are generally simpler models, using only one of these parameters.

$$f(\sigma, \theta, H_\alpha) < 0 \tag{6}$$

$$\sigma = \frac{\partial U}{\partial \varepsilon^{el}} \tag{7}$$

When the material is plastically flowing, the inelastic part of the deformation is defined by Eq. (8), where $g_i(\sigma, \theta, H_{i,\alpha})$ is the creep potential for the $\boldsymbol{i}$-th term of the system and $d\lambda_i$ is the range of time variation (dt). The way creep is described in Eq. (8), it is assumed that there is only one creep potential, g_i, in the i-system. More comprehensive plasticity models may present more than one creep potential at any given point.

$$d\varepsilon^{pl} = \sum d\lambda_i \frac{\partial g_i}{\partial \sigma} \tag{8}$$

For some rate-independent plasticity models, creep occurs in the same direction as the outer normal of the surface, according to Eq. (9), where $\boldsymbol{c_i}$ is a scalar.

$$\frac{\partial g_i}{\partial \sigma} = c_i \frac{\partial f_i}{\partial \sigma} \tag{9}$$

These plasticity models are called "associated creep" and are useful for materials where the deformation provides the necessary data on plastic creep when there are no changes in the plastic strain rate at a point. Metallic plasticity models (except for cast iron) use models of this type. The shape of the rate from associated creep models is essential to the theory of incremental plasticity, as it supports the modeling of the historical dependence of the response.

The last part that composes the plasticity model using Abaqus software is the set of evolution equations for the hardening parameters, which are represented in Eq. (10).

$$dH_{i,\alpha} = d\lambda_i h_{i,\alpha}(\sigma, \theta, H_{i,\beta}) \tag{10}$$

Where $h_{i,\alpha}$ is the hardening law (its variance) for $H_{i,\alpha}$. In complex plasticity models, which we can understand as for example, models used to somewhat describe the cyclic behavior of metals used for something like high temperature applications on parts, these evolution laws can sometimes present complicated forms. Since such high complexity is required to efficiently match the experimentally observed behavior in question. The model equations for such analyses presented in the Abaqus software use simple evolution equations: isotropic hardening, Prager-Ziegler kinematic hardening and the location of the center of the yield surface along the equivalent pressure axis in the Cam clay model. The independent form of the yield system proposed by the index i is implicit in the assumption of Eq. (10) represented above that the expected evolution of $H_{i,\alpha}$, is dependent only on one other parameter considered in the equation, which would be $H_{i,\beta}$, in the same (i-th) system.

At the end of all this walk through the plasticity models, it is understood that, from Eq. (2) to Eq. (10), the general structure presented for all plasticity models present in the Abaqus software is defined. Since the creep and hardening evolution rules are provided with a variance, they must be integrated to obtain the results.

3. RESULTS AND DISCUSSION

To begin this topic, we briefly highlight the possibility that this analysis allows, dividing the results into several frames to observe each detail that we want to give greater emphasis to enrich the analysis performed. To exemplify this issue, it can be seen in Figure 2 the instants of the displacements suffered by the tower under the influence of the Kobe Earthquake. It is worth emphasizing that the scales of the displacements are exaggerated for the purpose of better visualization.

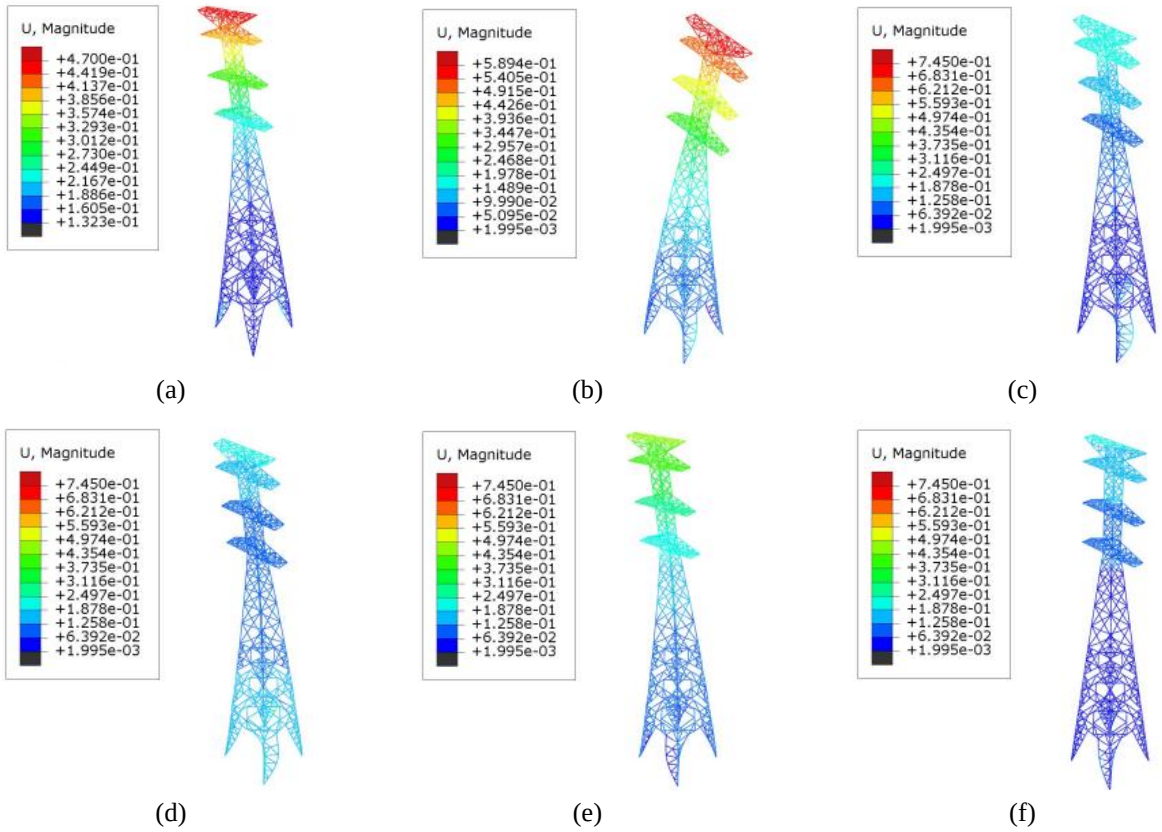

Figure 2. Example of the displacement of the tower as a result of the Kobe earthquake: (a) 10; (b) 20; (c) 30; (d) 40; (e) 50; (f) 60 (unit in seconds).

3.1 Pushover Analysis

The nonlinear static pushover analysis resulted in 151 frames, it was observed that the plasticization began near the links, lower part of the "legs" of the tower, passing quickly to the upper part, where the most critical area with accumulation of stresses and deformations is found, with a maximum plasticity value equal to 0.062 as shown in Figure 3. When the maximum plasticity occurs, causing the maximum load, it stabilizes for a brief moment until the computational analysis is aborted, which indicates the rupture of the most requested bar. In addition to its maximum load, the load under the tower prior to excessive deformations and failures can also be observed from the frames. The reactions at the supports of the tower structure were collected, thus representing the total resisted force, resulting in 457.25 kN, as well as the total top displacement, where they are presented in Graph 2. From Graph 2, and from a thorough analysis of the frames obtained, it was observed that the total force resisted by the elastic regime of the material was 102.51 kN at time 0.07 s of the analysis. This initial analysis is carried out to identify the total resistance of the constituent structure of the tower studied without any history of efforts on it, thus providing a basis for refining the subsequent analysis carried out and observing if, in fact, any significant loss will occur when affected before a static analysis like this.

3.2 Irpinia earthquake

Based on the accelerations presented in Graph 1(a), a peak acceleration of 0.17 m/s² (in modulus) was observed. Under the influence of these base accelerations, the tower suffered a maximum displacement at its top of 3.76 cm, as shown in Figure 4, at the instant 35.11 s of earthquake duration. Related to the maximum displacement is the maximum effort exerted on the tower, where a base reaction equal to 15.62 kN was obtained, as illustrated in Graph 3. It is important

to highlight that the maximum effort exerted corresponds to 15.24% of the total force resisted by the elastic regime, which prevented the occurrence of plastic deformation in the tower. In other words, the stresses in the structural elements caused by the influence of the earthquake analyzed, worked all the time with stresses lower than the yield strength of the steel used in the study. To further reaffirm this result, with a base displacement of 0.83 cm, a roof drift of 0.06% was obtained, a value that demonstrates the absence of extreme variations between the displacements that occurred in the tower. Thus, the energy tower structure studied presented an excellent performance in relation to the effects of the Irpinia Earthquake.

Turning now to the comparison between the referential pushover and residual pushover analyses, highlighted in Graph 4, it was observed that, as the accelerations used culminated at 15.24% of the elastic regime, and at 3.42% of the total resistance, the total residual resistance of the tower remained the same as obtained in the referential resistance, due to the little aggressive history, thus concluding that this earthquake was little influential for the tower studied.

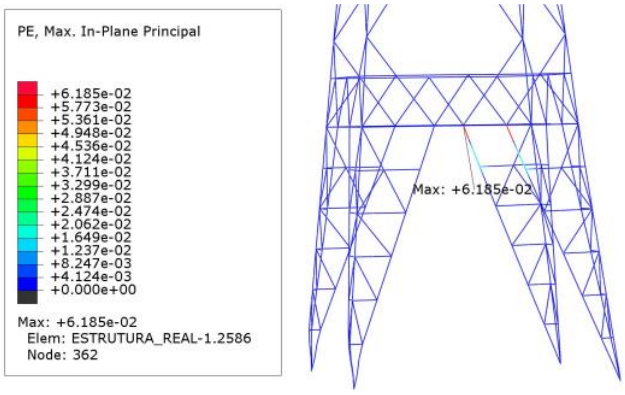

Figure 3. Maximum Plasticity of Reference Pushover (dimensionless).

Graph 2. Force x Displacement: Reference Pushover.

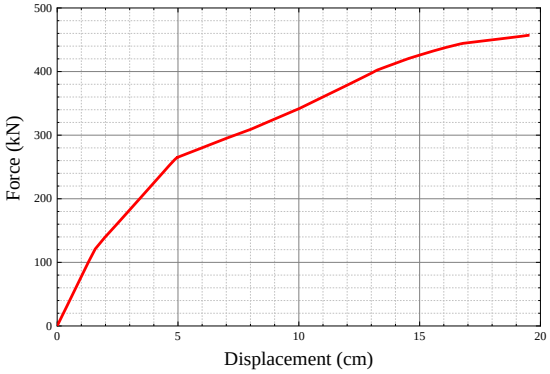

Graph 3. Irpinia's Base Reaction.

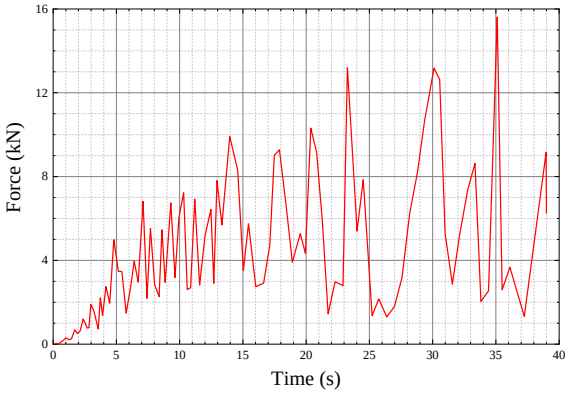

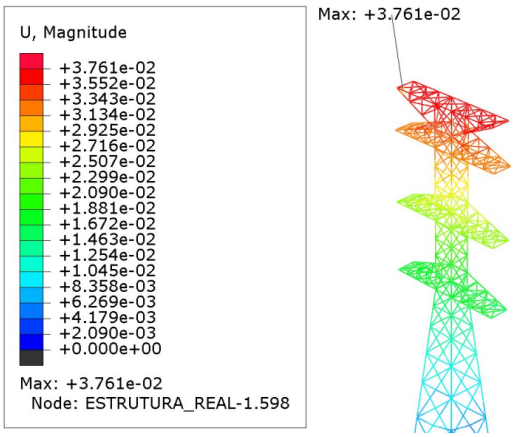

Figure 4. Irpinia's Max Displacement (unit in meters).

Graph 4. Irpinia comparison between referential and residual pushover.

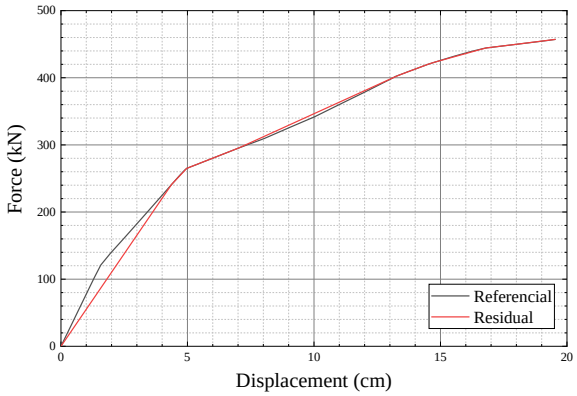

3.3 Kobe earthquake

Analyzing the accelerations presented in Graph 1(b), a peak acceleration of 2.11 m/s² (in module) was observed, as a result, the tower suffered a maximum displacement at its top of 71.74 cm, as shown in Figure 5, at the instant 28.36 s of the earthquake. Related to the maximum displacement is the maximum effort exerted, where a base reaction equal to 263.85 kN was obtained, as shown in Graph 5. Thus, based on the referential pushover analysis, it is noted that the tower is working in the plastic regime since its reaction is greater than the reaction supported by the elastic regime, also that it corresponds to 57.7% of the total resistance, however, the tower worked during the first 23 s of the earthquake in its elastic regime, and only after entering the plastic regime, and at 32.58 s, the model reached its maximum plasticity with a value of 0.002, illustrated in Figure 6. Looking at Graph 1(b), one can see that in the first 25 s of shaking the most active component is the vertical one, later the horizontal components begin to exert a greater effect on the tower and, as a result, the bars are occasionally less stressed in this way, and when the "whipping" of the tower begins to occur, the plasticity comes to the fore. But still, it can be considered that the tower performed well structurally in relation to the Kobe Earthquake as the plasticity received is 3.23% of the total plasticity the tower could withstand. With the tower experiencing a base displacement of 18.71 cm, the roof drift of 1.03% confirms the efficiency of the structural performance. An important point to highlight is that the plasticity occurred in different parts of the structure compared to Figures 3 and 6, this is due to the different request of the tower.

The result obtained from the comparison between the referential pushover and residual pushover analyzes is highlighted in Graph 6, it was observed that the residual pushover analysis started with a residual earthquake stress of 0.56 kN, a value that, although small, was discounted from the values obtained in the software, thus the residual resistance generated a value equal to 456.20 kN representing 99.77% of the referential resistance of the tower. This shows that the tower structure was affected by the excitations generated by the Kobe Earthquake, but the damage caused was somewhat insignificant.

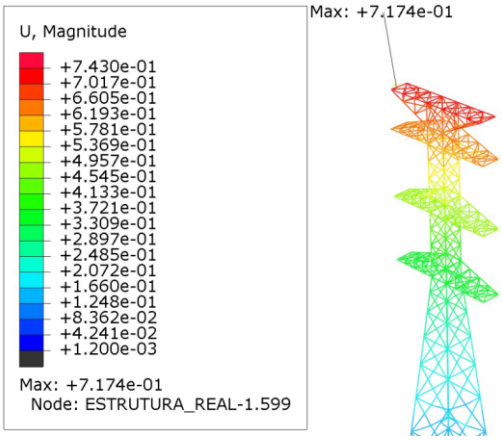

Figure 5. Kobe's Max Displacement (unit in meters).

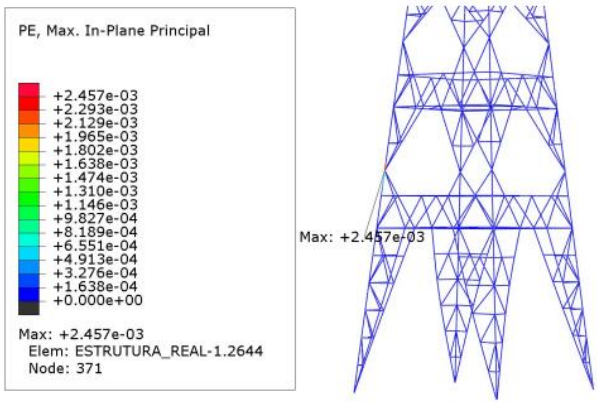

Figure 6: Kobe's Max Plasticity.

Graph 5. Kobe's Base Reaction.

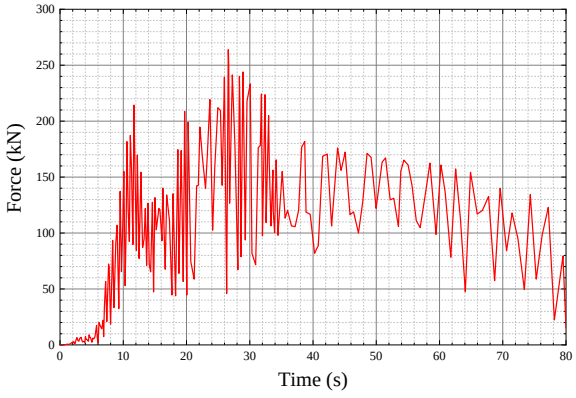

Graph 6. Kobe comparison between referential and residual pushover.

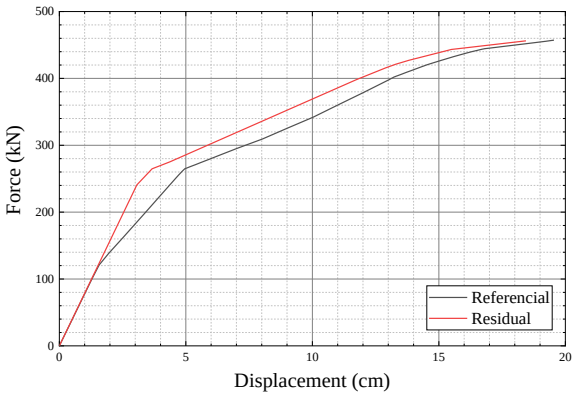

3.4 Loma Prieta earthquake

Turning now to the accelerations presented in Graph 1(c), a peak acceleration of 2.69 m/s² (in modulus) is observed. As a result of this, the tower suffered a maximum displacement at its top of 2.59 m as shown in Figure 7, at the instant 35.30 s of the earthquake. Related to the maximum displacement is the maximum effort exerted on the tower, where a base reaction equal to 255.32 kN was obtained, as shown in Graph 7, where it is complemented that it resulted in a slightly lower value in relation to the previous earthquake. Also noteworthy is the ratio of the maximum earthquake effort under the referential pushover analysis, corresponding to 55.84% of the total referential resistance. It should be noted that the tower showed plasticity due to the base excitations used, but as with the previous analysis, part of the earthquake duration generated only elastic deformations in the tower starting its plasticization at 7 s of the earthquake. After this moment, the plasticization occurred more incisively in two points of the tower structure, in the upper part near the lower stem of the tower, and in the lower part of the tower, illustrated in Figure 8. It should be emphasized in this analysis, as well as in the previous one, that plasticity occurred in different bars than in the referential pushover analysis. Also, in Figure 9 is mentioned the location and the maximum plasticity suffered with a value of 0.01. Considering the previous earthquake, it can be noted that although the base reaction of the Kobe Earthquake was greater compared to the current one, its effects were milder when compared to those of the Loma Prieta Earthquake, a fact that is related to the characteristic of the tremor. Observing Graph 1(c) and 1(b), it is noted that the accelerations of (c) are predominantly horizontal, while in (b) there is a greater distribution of the earthquake components, thus increasing the "whipping" of the tower and consequently the plasticity occurred. And it is also discussed that the plasticity occurred corresponds to 16.13% of the total plasticity occurred in the referential pushover analysis. Another point where the discrepancy is noted, even though the efforts are similar, is in the total top displacement that resulted in 2.59 m compared to the 74.83 cm suffered during the Kobe Earthquake. With a base displacement of 2.10 m, resulting in a roof drift of 0.95 %.

Comparing the referential pushover and residual pushover analyses, highlighted in Graph 8, it is noted that the residual pushover analysis started with an earthquake stress residue of 0.44 kN, as well as previously this value was discounted from the values obtained in the software, thus the residual resistance resulted in 452.04 kN, corresponding to 98.86% of the total referential resistance of the tower.

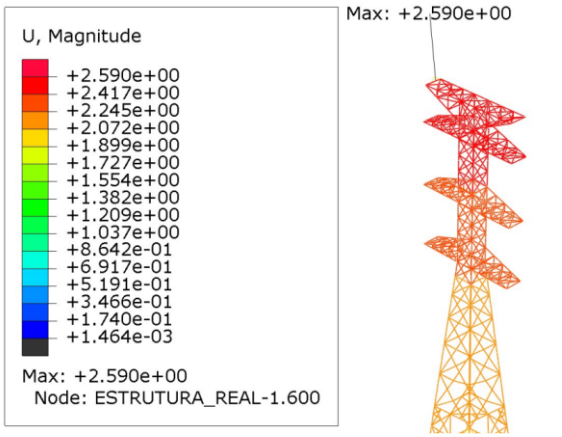

Figure 7. Loma Prieta's Max displacement (unit in meters).

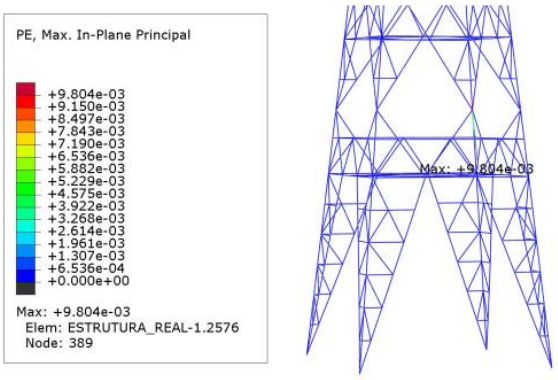

Figure 8. Loma Prieta's Max Plasticity (dimensionless).

Graph 7. Loma Prieta's Base Reaction.

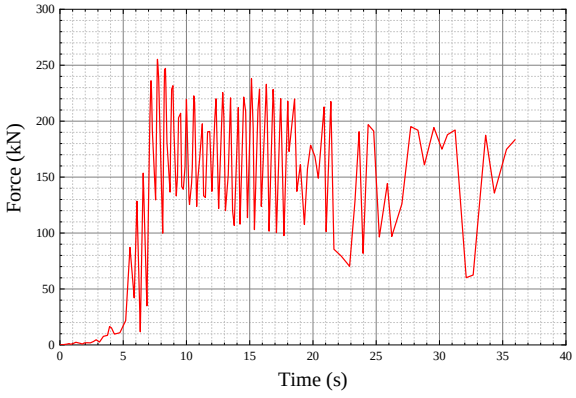

Graph 8. Comparison of Loma Prieta between referential and residual pushover.

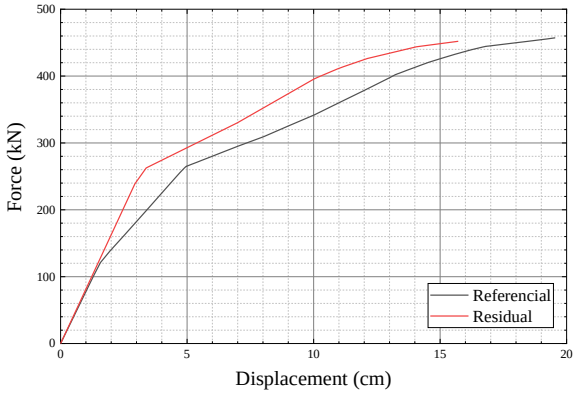

3.5 San Fernando earthquake

From the accelerations used in Graph 1(d), a peak acceleration of 2.17 m/s² (in modulus) was observed. From the efforts exerted by the accelerations, the maximum displacement at its top was 3.01 cm, but unlike the other earthquakes analyzed, the maximum total displacement of the tower did not occur at its top, but in the middle of the tower as shown in Figure 10, at the instant 10.68 s of the earthquake. Directly linked to the maximum displacement, there is the maximum effort that presents itself as a base reaction equal to 18.34 kN, as illustrated in Graph 9. Analyzing the maximum resistance presented in the referential pushover analysis, the requesting force of this earthquake corresponds to 4.01% of the total resistance supported by the tower, and 17.89% of the resistance of the elastic regime of the material. So, as in the Irpinia earthquake analysis, the tower worked in its entirety with elastic deformations, so no plastic deformation was recorded during the duration of the earthquake. To emphasize this result, suffering a base displacement of 1.73 cm, a roof drift of 0.02% was obtained, a value that demonstrates the absence of extreme variations between the displacements, resulting in an excellent performance in relation to the effects of the San Fernando Earthquake.

Moving now to the comparison between the referential pushover and residual pushover analyses, as well as at this point of the Irpinia Earthquake analysis, it is highlighted that as the accelerations used culminated at 17.89% of the elastic regime, and at 4.01% of the total resistance, the total residual resistance of the tower remained the same as that obtained in the referential resistance, with the little aggressive history, thus concluding that this earthquake was little influential for the studied tower.

Graph 9. San Fernando's Base Reaction.

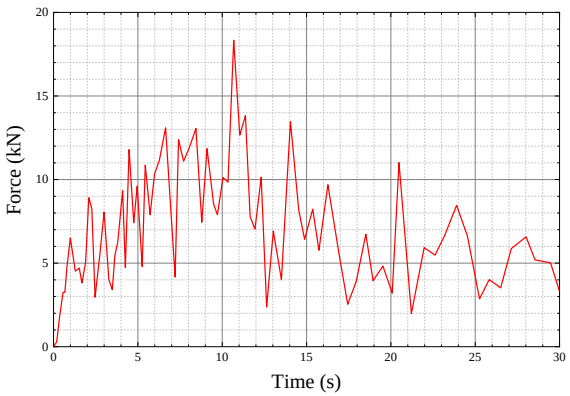

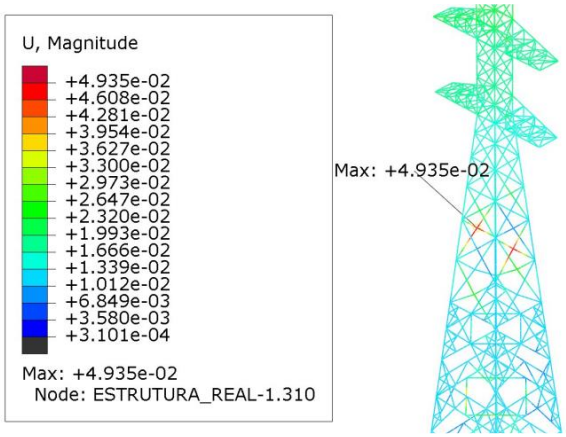

Figure 9. San Fernado's Max Displacement (unit in meters).

4. CONCLUSION

Based on the analyses performed, the tower showed good resistance in relation to all the three-dimensional excitations studied, no catastrophic failures occurred, however some bars were more stressed, and repairs or reinforcements should be foreseen with analyses like this. It should be noted that the most stressed members were different in the earthquakes as in the referential pushover analysis, a point to be considered since pushover analysis plays a large role in projects of this type. Due to the different earthquake types, it can be observed that the tower responses vary according to the intensity and direction of acceleration, but total force exerted on the tower can result in close values. It should also be noted that the history of request influences the loss of resistance over time as well as the loss of deformation capacity, as seen in the analysis of this article.

5. REFERENCE

BERNARD, Pascal; ZOLLO, Aldo. The Irpinia (Italy) 1980 earthquake: detailed analysis of a complex normal faulting. Journal of Geophysical Research: Solid Earth, v. 94, n. B2, p. 1631-1647, 1989.

CARLOS, Thiago Brazeiro et al. Dynamic analysis of guyed towers of transmission lines subjected to cable rupture. 2015.

DIETZ, Lynn D.; ELLSWORTH, William L. The October 17, 1989, Loma Prieta, California, earthquake and its aftershocks: Geometry of the sequence from high-resolution locations. Geophysical Research Letters, v. 17, n. 9, p. 1417-1420, 1990.

DOCUMENTATION, ABAQUS. Version 6.6, ABAQUS. 2006. Available at: https://classes.engineering.wustl.edu/2009/spring/mase5513/abaqus/docs/v6.6/index.html

GONTIJO, Carlos Roberto. Contribution to the analysis and design of self-supporting transmission line towers. 1994. (TOWER MODEL)

HORWICH, George. Economic lessons of the Kobe earthquake. Economic development and cultural change, v. 48, n. 3, p. 521-542, 2000.

PAN, Haiyang; LI, Chao; TIAN, Li. Seismic fragility analysis of transmission towers considering effects of soil-structure interaction and depth-varying ground motion inputs. Bulletin of Earthquake Engineering, v. 19, n. 11, p. 4311-4337, 2021.

PEER, NGA et al. Pacific earthquake engineering research center. PEER NGA Database, 2015.

TIAN, Li; LI, Hong Nan; WANG, Wen Ming. Response of Transmission Lines under Three-Dimensional Seismic Excitations. In: Applied Mechanics and Materials. Trans Tech Publications Ltd, 2012. p. 2259-2264.

WHITCOMB, James H. et al. San Fernando earthquake series, 1971: focal mechanisms and tectonics. Reviews of Geophysics, v. 11, n. 3, p. 693-730, 1973.

6. RESPONSIBILITY NOTE

The authors are the only responsible for the printed material included in this paper.